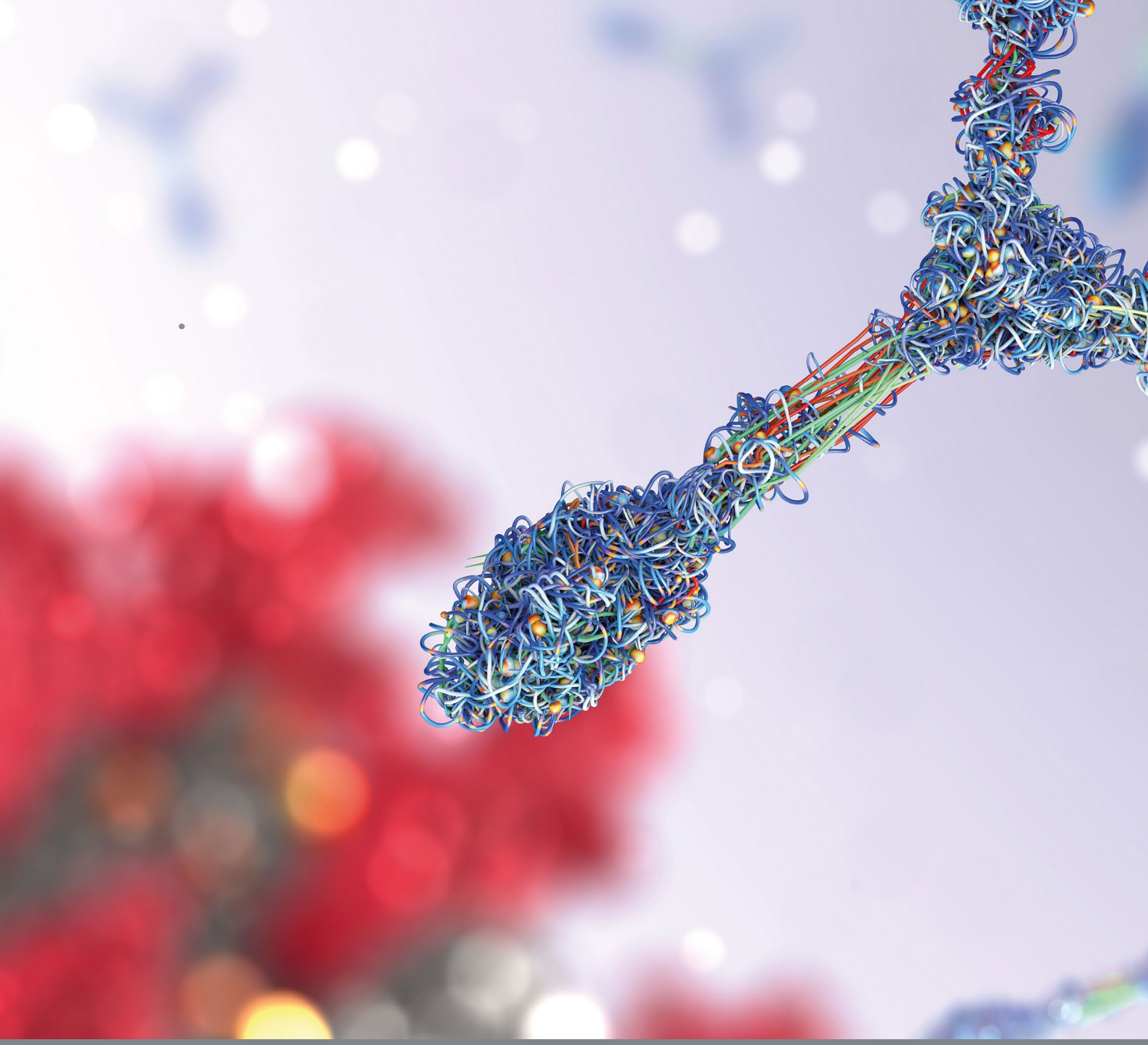

Enhancing Biomolecular Insights with Analytical Ultracentrifugation

Expert Insights

Sponsored by
BECKMAN COULTER Life Sciences
danaher
CURRENT PROTOCOLS
A Wiley Brand
WILEY

Contents

MULTIWAVELENGTH ANALYSIS WITH THE OPTIMA AUC ANALYTICAL ULTRACENTRIFUGE

The Optima AUC Analytical Ultracentrifuge with its new multiwavelength absorbance optics, resulting from decades of innovation and research at Beckman Coulter Life Sciences, has led to an entirely new generation of analytical ultracentrifuges, allowing for the in-depth and accurate characterization of viral vectors, LNPs, and interacting systems.
See for yourself.

- Viral vectors (e.g., AAVs)
- Empty, full, and partial capsid determination
- Nanoparticles (e.g., LNPs and EVs)
- Drug payload
- Protein interactions
- Enzymes and other proteins

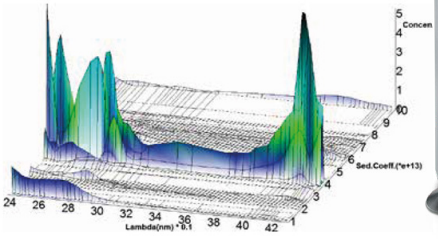

BECKMAN COULTER Life Sciences

For Beckman Coulter's worldwide office locations and phone numbers, please visit Contact Us at beckman.com

2024-GBL-EN-105880-v1

danaher

Introduction

Analytical ultracentrifugation (AUC) serves as a vital technique in medicinal research, offering critical insights into the characterization of macromolecules such as proteins, lipid nanoparticles (LNPs), viral vectors, nucleic acids, and other biological assemblies. As the field of medicine advances, there is an increasing need for precise and reliable analytical methods to understand complex biological interactions and develop effective therapeutic strategies. Recent innovations in AUC technology have enhanced its precision, efficiency, and applicability, making it an indispensable tool for bioanalysis. This collection of expert insights explores the transformative impact of modern AUC techniques on advancing research and therapeutic development, highlighting its role in addressing contemporary challenges and driving innovation.

This Expert Insights begins with a study by McAlpine *et al.* [1], which reports the discovery of ubiquitin variants (UbVs) that inhibit the E2 enzyme Ube2d2. The researchers utilized AUC to investigate the interactions between UbVs and the E2 enzyme, offering insights into novel therapeutic strategies for diseases involving ubiquitin system disruptions.

Next, Erlandsen *et al.* [2] explore the binding and assembly properties of CtBP1 and CtBP2. Utilizing AUC, the study demonstrates that CtBP proteins form tetramers in the presence of NAD+ or NADH, with tetramer to dimer dissociation constants around 100 nM. This research reveals NAD(H) binding affinities, suggesting that CtBP proteins are fully saturated with NAD+ under physiological conditions, thereby challenging their role as NADH sensors.

This digest is followed by an interview with Dr. Alexander Bepperling, Sandoz, highlighting how AUC can be used in analyzing biopharmaceutical formulations.

Next, an application note by Henrickson provides an in-depth review of the use of AUC for the characterization of lipid nanoparticles (LNPs). The note emphasizes the advantages of LNPs, such as improved stability and adaptability, and highlights how AUC contributes to understanding their structural and functional properties, thereby facilitating the development of effective therapeutic delivery systems.

Finally, the whitepaper by Henrickson and Qureshi discusses the use of multiwavelength analytical ultracentrifugation (MW-AUC) for studying biopolymer interactions. It emphasizes the advantages of MW-AUC, such as high-resolution characterization and the ability to differentiate analytes based on their absorbance spectra. The paper demonstrates how MW-AUC enhances molecular studies by accurately elucidating complex interactions, driving advancements in biopharmaceuticals.

These studies highlight the pivotal role of analytical ultracentrifugation in advancing biotherapeutic research, showcasing innovations that significantly enhance accuracy and understanding.

Through the methods and applications presented here, we aim to educate researchers on the latest advancements in analytical ultracentrifugation for medicinal applications. To gain a deeper understanding of available options for improving your research, we encourage you to visit Beckman Coulter's website.

Dr. Christene A. Smith
Editor at Wiley

References

[1] McAlpine, J.M.R.B. *et al.* (2024). Structural and biophysical characterisation of ubiquitin variants that inhibit the ubiquitin conjugating enzyme Ube2d2. *The FEBS Journal*. https://doi.org/10.1111/febs.17311.

[2] Erlandsen, H. *et al.* (2022). NADH/NAD+ binding and linked tetrameric assembly of the oncogenic transcription factors CtBP1 and CtBP2. *FEBS Letters*. https://doi.org/10.1002/1873-3468.14276.

Structural and Biophysical Characterisation of Ubiquitin Variants that Inhibit the Ubiquitin Conjugating Enzyme Ube2d2

Adapted from J. M. R. B. McAlpine *et al.*

Introduction

Protein modification with ubiquitin is essential for various eukaryotic cellular functions, including protein degradation, cell signaling, and DNA packaging. This modification process involves a cascade of three enzymes: E1, E2, and E3, with E2 enzymes playing a crucial role in determining the type of ubiquitin chain formed. The Ube2d family of E2 enzymes is particularly important, as it is involved in DNA repair and the regulation of apoptosis. These enzymes bind ubiquitin non-covalently at a 'backside' site, which enhances their ability to form ubiquitin chains. Disruptions in ubiquitin modification can lead to diseases such as cancer and neurodegenerative disorders.

A library of ubiquitin variants (UbVs) was created to modulate the ubiquitin system, leading to the discovery of UbVs that can decrease ubiquitin transfer activity by binding to E2 enzymes. Using phage display, McAlpine and colleagues identified UbVs that bind to Ube2d2 at sites distinct from the backside, effectively inhibiting ubiquitin chain formation. Crystallographic and biophysical analyses showed that these UbVs disrupt interactions with the E1 enzyme, and one UbV binds more weakly at an additional site overlapping with the backside, enhancing its inhibitory effect. These findings highlight the potential for developing compounds that specifically target and impede the activity of distinct E2 enzymes, offering new avenues for therapeutic interventions.

Methodology

Engineering Ubiquitin Variants

Ube2d2^{S22R} and related proteins were cloned into various vectors for expression in *E. coli* BL21 (DE3) cells. The proteins were expressed with either a cleavable His-tag or GST tag, followed by purification using nickel-affinity or Glutathione Sepharose 4B chromatography. The proteins were then concentrated, flash-frozen, and stored at -80 °C. Ube2d2^{S22R}-Avi was biotinylated using BirA.

Phage display was conducted by immobilizing biotinylated Ube2d2^{S22R} onto streptavidin or neutravidin-coated 96-well plates, followed by four rounds of binding selection to screen 96 clones using ELISA, resulting in the selection of six UbVs for further investigation. These UbVs were then used in various in vitro assays to explore their binding and functional interactions with Ube2d2.

Analytical Ultracentrifugation

Sedimentation velocity (SV) experiments were performed using the Optima AUC (Beckman Coulter, Auckland, New Zealand) with an AN-50 Ti Rotor to analyze the solution characteristics of proteins, including UbV.1, UbV.3, Ube2d2, and Ube2d2^{S22R}, at 25 °C in PBS. Data were collected at 50,000 r.p.m. and analyzed with UltraScan 4.0 using two-dimensional spectrum analysis (2DSA) and genetic algorithm regularization, achieving a good fit by removing noise and fitting boundary conditions.

Results

The researchers began by selecting ubiquitin variants (UbVs) against a mutant form of Ube2d2, known as Ube2d2^{S22R}, which contains a mutation that disrupts backside ubiquitin binding. Through phage display, six UbVs were identified, with UbV.1 and UbV.3 showing significant inhibitory effects on ubiquitin chain-building activity. The UbVs were shown to inhibit the formation of ubiquitin chains by interfering with the charging of Ube2d2, effectively reducing its interaction with the E1 enzyme, as confirmed by SDS/PAGE analysis (Fig. 1C).

Crystal structures of UbV.1 with Ube2d2 and UbV.3 with Ube2d2^{S22R} were solved, revealing that these UbVs form stable complexes with the E2 enzyme. The structures showed that UbV.1 binds to two sites on Ube2d2, while UbV.3 binds at a single site, with both variants disrupting critical protein–protein interactions necessary for ubiquitin chain formation. Isothermal titration calorimetry (ITC) confirmed that both UbVs form stable complexes with Ube2d2 and Ube2d2^{S22R}, although with different stoichiometry, highlighting the binding dynamics of these interactions.

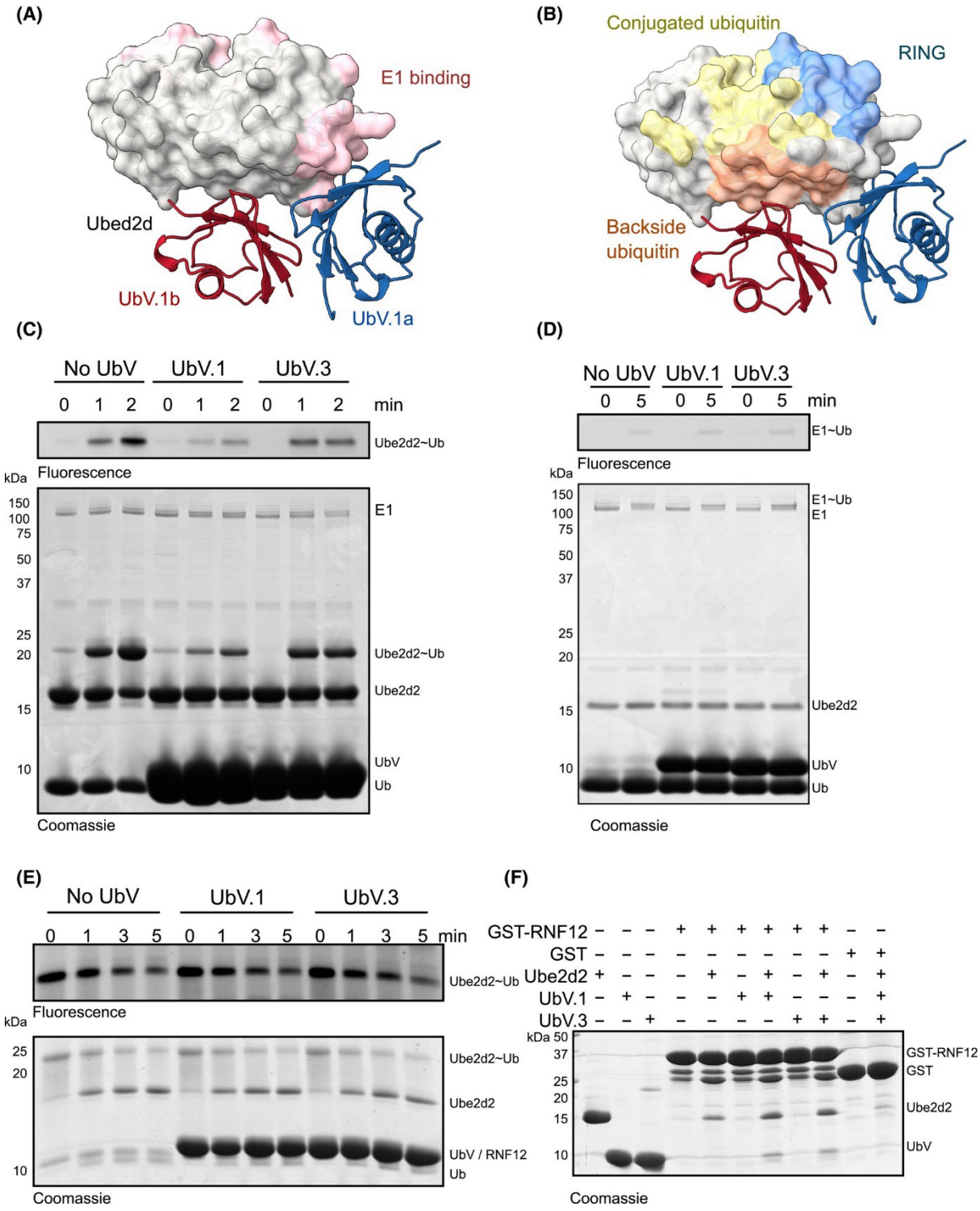

Figure 1. Functional analysis of the UbV-Ube2d2 complexes. (A, B) A surface representation of Ube2d2 in grey with UbV.1a in blue and UbV.1b in red. Panels indicate the interface with: (A) the E1 enzyme in pink (PDB: 7K5J); **(B)** the RING interface in blue, the conjugated ubiquitin interface in yellow, and the allosteric backside binding site in orange (PDB: 4V3L). UbV.3 is not shown for clarity. **(C)** A single-turnover E2 charging assay showing the formation of the Ube2d2~Ubiquitin conjugate with or without the two UbVs. **(D)** An E1 activating assay with or without the two UbVs. **(E)** A single-turnover E3-catalysed ubiquitin discharge of Ube2d2~Ubiquitin conjugates with or without the UbVs. Assays were done in triplicate, and representative gels are shown. Gels were imaged at 600 nm and stained with Coomassie die. **(F)** A pulldown experiment comparing binding of GST-RNF12RING to Ube2d2 with or without the UbVs.

Analytical ultracentrifugation was used to study the interactions between ubiquitin variants (UbVs) and the E2 enzyme Ube2d2 and its mutant form, UBe2d2^{S22R}, and to confirm the crystallography results in solution. Sedimentation velocity analysis revealed that when UbVs were mixed with the E2 enzymes, there were shifts in sedimentation peaks, indicating complex formation.

The UbV.1-Ube2d2 complex showed a peak at 2.87 S, suggesting one or two UbV.1 molecules bind to Ube2d2. In contrast, the UbV.1-Ube2d2^{S22R} complex showed a smaller shift, indicating weaker binding (Fig. 2D). These findings were consistent with ITC and size-exclusion chromatography results, confirming stable complex formation and providing insights into binding dynamics (Fig. 2A, B).

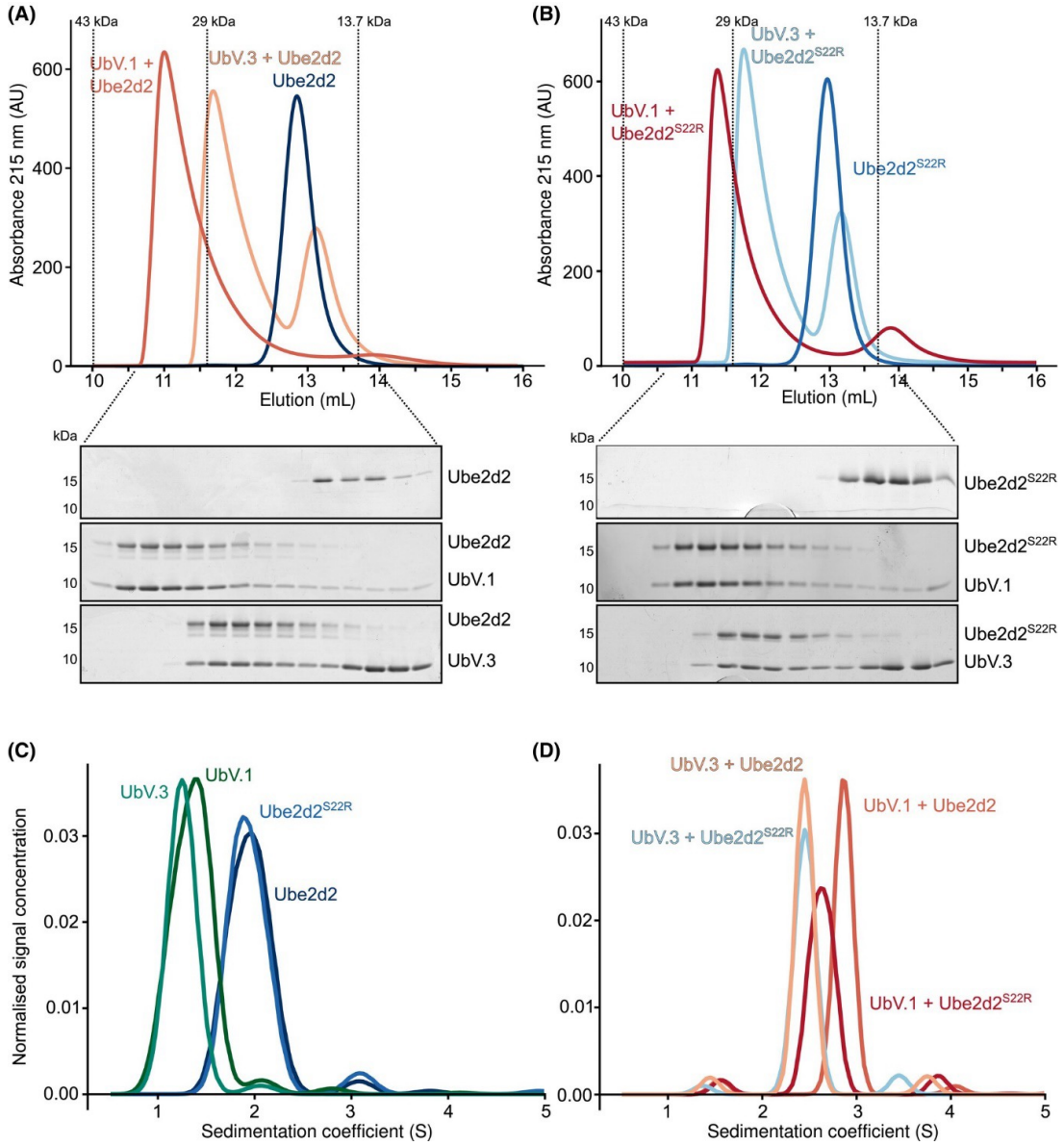

Figure 2: Determining the stoichiometry of the UbV-Ube2d2 complexes in solution. (A, B) Size-exclusion chromatography of UbV.1 and UbV.3 with **(A)** Ube2d2 and **(B)** Ube2d2^{S22R}. Below shows the corresponding fractions. The formation of stable complexes is indicated by elution peaks shifting to the left. Protein standards were used to determine the molecular weights indicated with dotted lines. **(C)** Sedimentation velocity analysis of Ube2d2, Ube2d2^{S22R}, UbV.1 and UbV.3 alone (detected at 280 nm). **(D)** Sedimentation velocity analysis of UbV-Ube2d2 complexes where Ube2d2 and Ube2d2^{S22R} were labelled with fluorescein isothiocyanate (FITC) and sedimentation tracked using the absorbance of FITC at 493 nm. As a result, only Ube2d2 and Ube2d2^{S22R} can be observed. Stable complexes are indicated by peak shifts to the right relative to panel C.

Discussion

The study successfully identified ubiquitin variants (UbVs) that specifically inhibit the E2 enzyme Ube2d2, with a combination of techniques providing insights into their interactions. AUC showed consistent results with ITC and SEC, and confirmed the formation of stable complexes between UbVs and Ube2d2. AUC determined that the UbV.1-Ube2d2 complex has two binding sites with different affinities, and that the UbV.1-Ube2d2^{S22R} complex has a stoichiometry closer to one UbV.1 molecule per Ube2d2^{S22R} molecule. It was observed that UbV.1 binds with different affinities to Ube2d2 and its mutant form, Ube2d2^{S22R}, indicating specific protein-protein interactions within the ubiquitin-proteasome system.

The findings suggest potential applications for developing targeted inhibitors of E2 enzymes. By leveraging structural insights from these techniques, researchers can design UbVs with enhanced binding affinities and specificities, opening avenues for novel therapeutic strategies. Moreover, the ability of UbVs to selectively modulate the activity of closely related E2 enzymes within the Ube2d family highlights their utility as research tools for investigating the distinct biological roles of these enzymes.

References

[1] Osborne, H.C. *et al.* (2021). E2 enzymes in genome stability: pulling the strings behind the scenes. *Trends in Cell Biology.* https://doi.org/10.1016/j.tcb.2021.01.009.

NADH/NAD+ Binding and Linked Tetrameric Assembly of the Oncogenic Transcription Factors CtBP1 and CtBP2

Adapted from H. Erlandsen *et al.*

Introduction

C-terminal binding proteins (CtBP1 and CtBP2) are paralogs that influence cell fate through transcriptional activity, initially identified by their interaction with the adenovirus E1A oncoprotein. CtBP recruits chromatin remodeling enzymes to transcription factors, affecting processes like apoptosis and the epithelial phenotype. It represses genes like cell cycle inhibitors and proapoptotic factors, while activating growth and metastasis-related genes, promoting epithelial-to-mesenchymal transition. CtBP is upregulated in various cancers, correlating with increased mortality, and mouse models show its role in cancer progression.

CtBP's oligomerization, influenced by NAD(H) binding, is crucial for its transcriptional activity. Though NAD(H) is known to trigger CtBP assembly, whether it forms dimers or tetramers remains debated. Studies suggest NADH has a higher affinity than NAD+, implying CtBP acts as a metabolic sensor. Using analytical ultracentrifugation (AUC) and isothermal titration calorimetry, the authors found CtBP1 and CtBP2 predominantly form stable tetramers in solution with NAD(H). The dissociation constants for NAD(H) binding indicate CtBP is nearly fully saturated with NAD+ in normal cellular conditions, challenging its role as an NADH sensor.

Methodology

Expression and Purification of CtBP1 and CtBP2

The expression and purification of CtBP1 (28–440) and CtBP2 (31–445) were carried out using established protocols [1–3]. The proteins were expressed in bacterial systems and purified through a series of chromatographic steps. The final purification involved a size exclusion column, conducted at 4 °C with specific buffers supplemented with NAD+, AMP, or no nucleotide, depending on the experimental requirements. This step was crucial to ensure the removal of any bound NAD(H), allowing for accurate analysis of the protein's oligomerization state.

Analytical Ultracentrifugation

Analytical ultracentrifugation was used to study the sedimentation behavior of CtBP1 and CtBP2. Sedimentation velocity (SV) and sedimentation equilibrium (SE) analyses were performed to determine the dissociation constants for the dimer-tetramer equilibrium. The experiments were conducted using two-channel aluminum-Epon double-sector centerpieces and quartz windows. Absorbance data were collected in a Beckman Coulter Optima AUC analytical ultracentrifuge operating at 35,000 r.p.m. and 20 °C. The c(s) distributions were calculated using SEDFIT, providing insights into the protein's oligomerization state under different conditions. Measurements were taken at 280 nm for the protein and 340 nm for NADH allowed for selective monitoring of each component, enabling precise tracking of the protein's behavior and interactions at 280 nm while simultaneously observing the specific activity and binding characteristics of NADH at 340 nm.

Isothermal Titration Calorimetry (ITC)

Isothermal titration calorimetry was employed to measure the binding affinity of NAD(H) to CtBP1 and CtBP2. CtBP1 and CtBP2 were less stable in the absence NAD(H), therefore calorimetry was performed immediately following column elution. The experiments were conducted at 23 °C. Protein samples were prepared in a buffer containing 50 mM HEPES pH 7.5, 300 mM NaCl, 5 mM EDTA, and 2 mM TCEP. The binding experiments involved titrating NADH or NAD+ into the protein solution and measuring the heat change associated with binding. Data were analyzed to determine the thermodynamic parameters of binding, including the dissociation constant (K_d), enthalpy change (ΔH), and entropy change (ΔS).

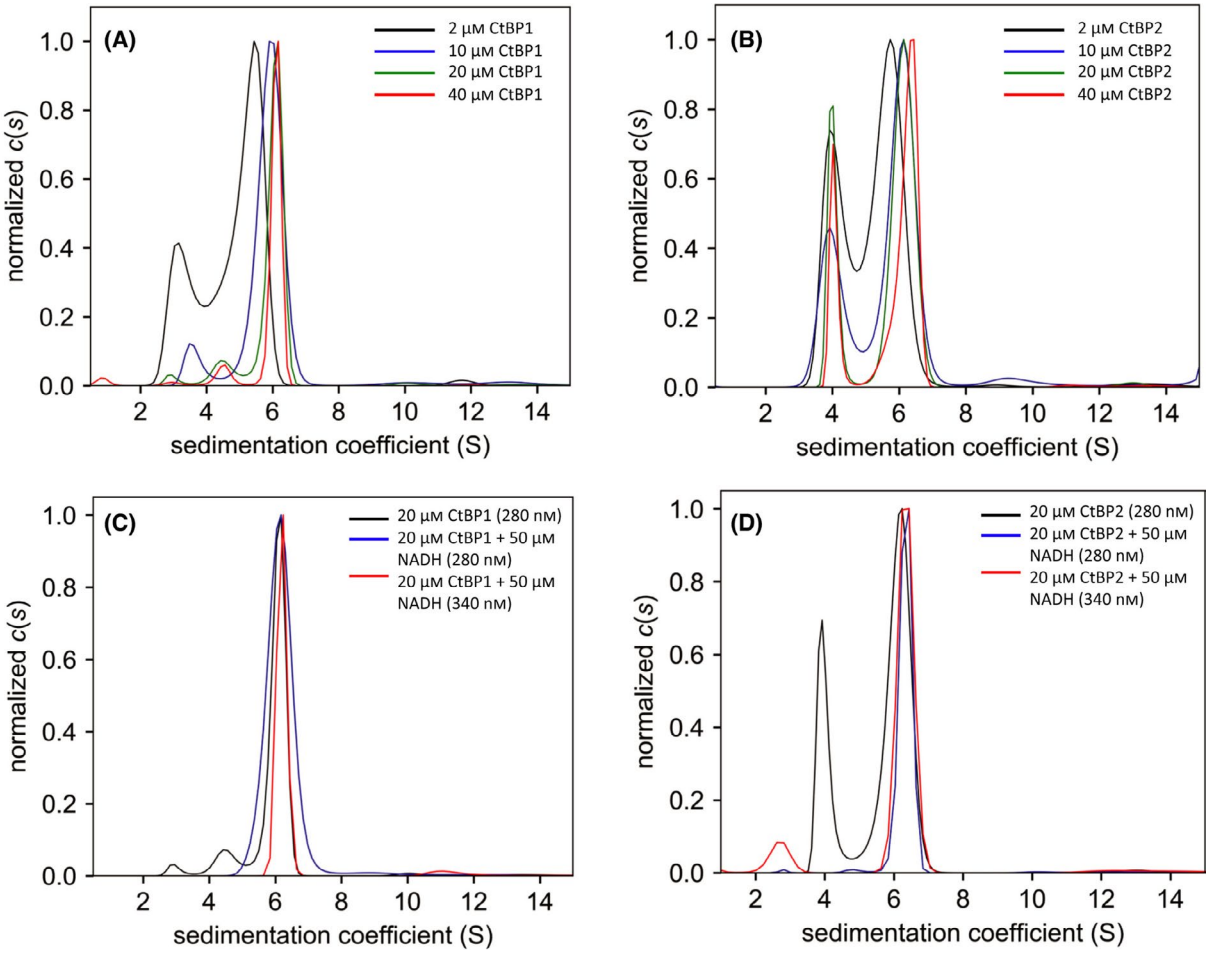

Figure 1: Sedimentation velocity analysis of CtBP1 and CtBP2 self-association. (A) c(s) distribution of CtBP1 as purified [no added NAD(H); at 2, 10, 20 and 40 µM (monomer equivalents)]; **(B)** c(s) distributions of CtBP2 as purified (no added NAD(H); at 2, 10, 20 and 40 µM); **(C)** 20 µM CtBP1 as purified (no added NAD(H)) compared to CtBP1 with 50 µM NADH at 280 and 340 nm wavelength (340 nm/NADH signal is red) and **(D)** 20 µM CtBP2 as purified (no added NAD(H)) compared to CtBP2 with 50 µM NADH at 280 and 340 nm wavelength (340 nm/NADH signal is red). All of the distributions are normalized by maximum peak height.

Results and Discussion

Dimer-Tetramer Equilibrium

The SV analysis of CtBP1 and CtBP2 without added nucleotide showed a dominant peak near 6 S (Fig. 1a, b). This peak shifts slightly to the left when the protein concentration is decreased from 40 to 2 µM, which implies the peak corresponds to a reaction boundary associated with rapid reversible self-association. Both proteins also presented additional peaks at lower sedimentation coefficients which were not present in SV AUC experiments when NADH was added (Fig. 1c, d), though the 6 S peak remained. The researchers assign the lower s peaks to apoprotein and the 6 S peaks to the NADH complexes. The assignment was demonstrated through the use of multiwavelengths, as tracking the sedimentation at 340 nm showed that NADH co-sedimented with the 6 S peak. They speculate that the 6 S peak present with no added nucleotide indicates that some NAD+ remained in the purified proteins or another adenine nucleotide species.

Due to the variability and reversible self-association of CtBP1 and CtBP2, reliable molecular masses could not be derived from SV data, leading to the use of sedimentation equilibrium (SE) AUC measurements. These measurements indicated negligible tetramer dissociation over a concentration range of 3–13 µM with 50 µM NAD(H), confirming a tetrameric structure with a molecular mass of 192.1 kDa (Fig. 2). This finding aligns with previous analyses, indicating that the SV peak near 6 S corresponds to tetramers, while the 4.1 S feature is attributed to dimers. Both forms exhibit a frictional ratio of about 1.6, consistent with substantial disordered regions due to the inclusion of ~90 unstructured C-terminal residues.

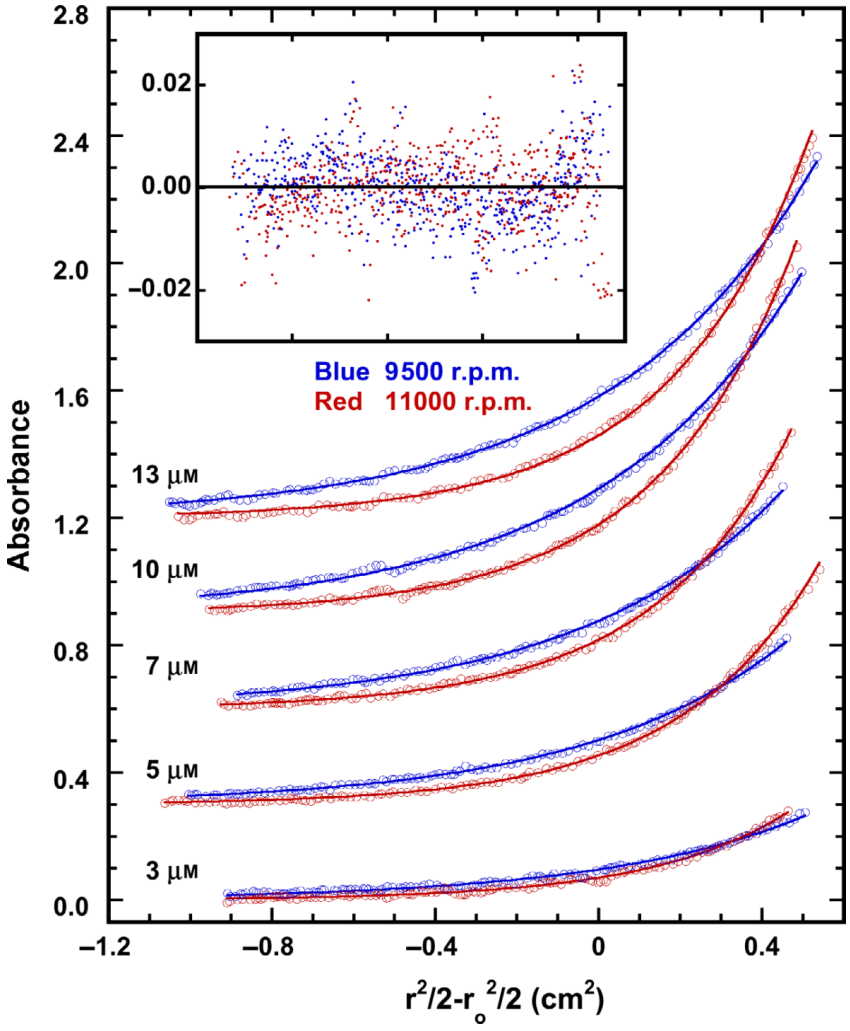

Figure 2: Sedimentation equilibrium analysis of CtBP2 self-association in the presence of 50 µM NADH. Data (open circles) were collected at five protein concentrations ranging from 3 to 13 µM with 50 µM NADH at two rotor speeds: 9500 r.p.m. (blue) and 11 000 r.p.m. (red) at a wavelength of 280 nm.

In the presence of either NADH or NAD+, both CtBP1 and CtBP2 predominantly form tetramers at concentrations of 2 µM and above. However, SV analysis reveals that as the concentration decreases, some dissociation into dimers occurs. Due to the weak absorbance of protein aromatic side chains at 280 nm, the researchers utilized the peptide backbone absorption at 230 nm for enhanced sensitivity in characterizing the dimer-tetramer equilibrium.

The study highlighted that weight-average sedimentation coefficients (s_w) were obtained through SV AUC titrations ranging from 300 nM to 5 µM. This data revealed that for both proteins, CtBP1 and CtBP2, the s_w increased from approximately 5.4 to 6.1 S over this concentration range.

The data was then fit to dimer-tetramer equilibrium models to obtain dissociation constants (Kd values), which are displayed in Fig. 2. This approach provided a clear understanding of the concentration-dependent dissociation behavior of CtBP tetramers.

AUC results provide definitive proof that CtBP1 and CtBP2 assemble into tetramers in the presence of NAD(H) (Fig. 2), despite the common assumption that NAD(H) triggers a monomer-to-dimer assembly. This result suggests that sedimentation experiments could be an important assay to investigate the ability of various CtBP inhibitors to directly disrupt transcriptionally dependent CtBP tetramer formation.

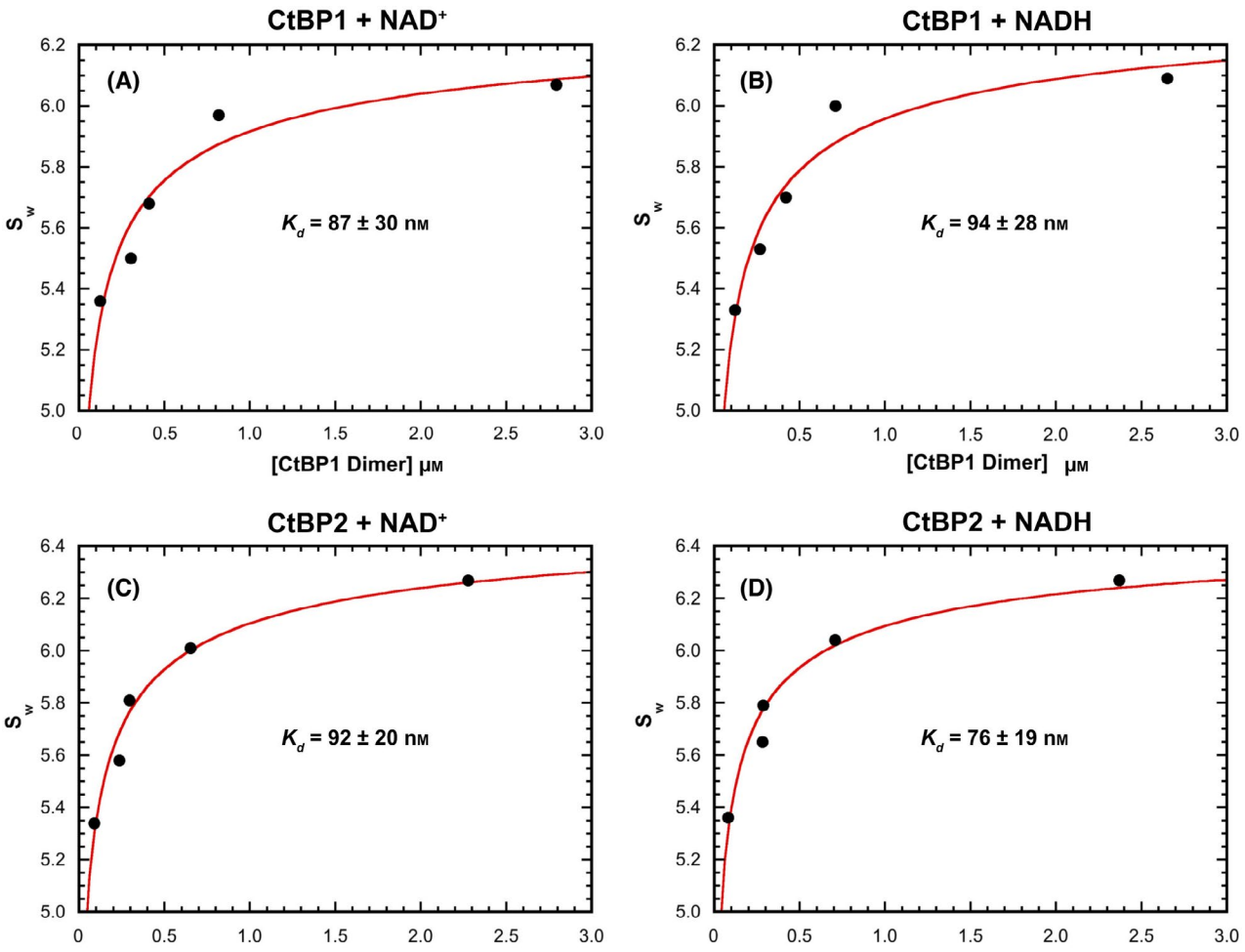

Figure 3. Determination of CtBP1 and CtBP2 dissociation constants: weight-average sedimentation coefficient analysis. (A) CtBP1 + NAD+; **(B)** CtBP1 + NADH; **(C)** CtBP2 + NAD+; **(D)** CtBP2 + NADH.

Binding Affinity of NAD(H)

ITC results revealed that CtBP1 binds NADH with a K_d of 53 ± 14 nM, while its affinity for NAD+ is about 9 times weaker, with a K_d of 450 ± 43 nM. CtBP2, although less stable without a bound nucleotide, binds NAD+ more tightly than CtBP1. For CtBP2, the K_d for NADH is 31 ± 6 nM, and its binding to NAD+ is nearly two-fold weaker, with a K_d of 51 ± 15 nM.

CtBP2 tetramers are more stable than CtBP1, potentially explaining their higher affinity, as a larger portion of CtBP2 remains tetrameric without nucleotides. SV analysis shows about 90% of CtBP2 and 60% of CtBP1 are tetrameric at 40 µM. Attempts to estimate NAD(H) affinity in CtBP1 dimers below 10 µM using ITC were unsuccessful. The results confirm that NADH binds more tightly to CtBP than NAD+, but the difference is much smaller than the previously suggested 100-fold [4].

Conclusions

The findings of this study have significant implications for understanding the role of CtBP in cellular metabolism and gene regulation. The predominance of the tetrameric form suggests that CtBP's repressor activity is linked to its oligomerization state. The binding of NAD(H) not only influences the structural configuration of CtBP but also its interaction with other proteins and DNA. These insights contribute to a better understanding of CtBP's function as a transcriptional corepressor and its involvement in metabolic pathways.

This study provides definitive evidence that CtBP1 and CtBP2 assemble into tetramers in the presence of NAD(H), challenging previous assumptions of a monomer-to-dimer transition. AUC played a crucial role, with sedimentation equilibrium (SE) measurements unambiguously demonstrating this tetramer formation.

AUC and ITC confirm that nucleotide binding is thermodynamically linked to the assembly of dimers into tetramers, with dissociation constants indicating strong binding affinity. These findings have significant implications for understanding the role of CtBP in cancer progression and developing inhibitors to disrupt its transcriptional activity. While previous hypotheses suggested CtBP could act as a metabolic sensor by detecting NADH levels, the study's results indicate that CtBP is nearly fully saturated with NAD+ under physiological conditions, arguing against this sensor role. The research highlights the importance of AUC experiments in evaluating CtBP inhibitors' effectiveness in disrupting tetramer formation, offering valuable insights into potential therapeutic strategies.

The research challenges previous assumptions about CtBP's oligomerization and highlights the importance of NAD(H) binding in regulating its function. These findings have significant implications for understanding CtBP's role in cellular metabolism and gene regulation, offering new perspectives on its potential as a therapeutic target.

References

[1] Bellesis, A.G. *et al*. (2018). Assembly of human C-terminal binding protein (CtBP) into tetramers. *Journal of Biological Chemistry*. https://doi.org/10.1074/jbc.RA118.002514.

[2] Hilbert, B.J. *et al*. (2015). Structure-guided design of a high affinity inhibitor to human CtBP. *ACS Chemical Biology*. https://doi.org/10.1021/cb500820b.

[3] Nichols, J.C. *et al*. (2021). NAD(H) phosphates mediate tetramer assembly of human C-Terminal binding protein (CtBP). *Journal of Biological Chemistry*. https://doi.org/10.1016/j.jbc.2021.100351.

[4] Fjeld, C.C. *et al*. (2003). Differential binding of NAD+ and NADH allows the transcriptional corepressor carboxyl-terminal binding protein to serve as a metabolic sensor. *Proceedings of the National Academy of Sciences of the United States of America*. https://doi.org/10.1073/pnas.1633591100.

Analyzing Biopharmaceutical Formulations

Interview with Dr. Alexander Bepperling

In this interview, Dr. Alexander Bepperling, Sr. Manager Analytical Characterization, Sandoz, discusses his research on high-concentration biopharmaceutical formulations using Analytical Ultracentrifugation (AUC). He highlights the importance of analyzing biopharmaceuticals in their native state for accurate stability and aggregation predictions. Dr. Bepperling explains advancements in AUC techniques and shares insights from his research. He also explores the future potential of AUC in advancing biopharmaceutical development. This interview offers an in-depth look at the transformative impact of AUC on the industry.

Professional Experience:

Could you please introduce yourself and share a bit about your professional background and experience in the field of biopharmaceutical research?

Hi, my name is Alexander Bepperling.

I'm currently running a biophysical characterization lab at Sandoz. I joined the company when it was still under the name Novartis, following a spin-off to Sandoz in 2023. When I started, I was primarily responsible for binding technology, mainly SPR (surface plasmon resonance), and the measurement of higher-order structures. During my PhD, I came into contact with analytical ultracentrifugation (AUC), and in 2012, Novartis invested in that direction. I built up the respective lab, and since then, I have been the main expert for AUC at Hexal Sandoz, Novartis.

AUC and Characterization of Biopharmaceuticals:

Can you explain what Analytical Ultracentrifugation (AUC) is and why it's important in biopharmaceutical research?

First of all, it's an orthogonal technique mentioned by several guidelines of the FDA and EMA for the determination of aggregates. That's, I think, the reason why every company has one.

The second reason emerged a few years ago when cell and gene therapy came into the picture. They provide a unique challenge because they are very, very large molecules, much larger than traditional biopharmaceuticals, including antibodies, growth hormones, or other similarly derived proteins. For AUC, you can say the larger the molecule, the better the resolution. For things like AAV, it even became a release method, which is really a boost for the field.

What are some of the different applications or therapeutics that AUC has helped you analyze?

Besides the conventional antibody format, we are also diving more and more into the area of siRNA and antisense oligonucleotides. Here, AUC is particularly valuable because it can distinguish between the sense and antisense strands, for example. Even if they have roughly identical sizes, they have different hydrodynamic properties. You also have the possibility to analyze the loading of lipid nanoparticles (LNPs).

When we talk about high-concentration AUC, there are more and more patents coming out that describe the oligomeric distribution as part of the patent. This means if you develop a biosimilar or generic drug, you need to match this distribution. A famous example may be the peptides used for weight loss, such as Tirzepatide, which may also be well known in public media. For these, the oligomeric distribution for each of the six strengths is described in the patent, and they range from 5 to 30 mg/ml. You need to cover all that and measure it as it is without prior dilution. AUC is, I would say, the only method really able to provide you with a size distribution of the undiluted drug.

What are the challenges of working with high-concentration formulations of biopharmaceuticals, and why is it important to study them in their original form? How does AUC compare to orthogonal technologies for high-concentration formulations which are traditionally very difficult to analyze?

If we talk about difficulties, there are two main challenges. The first one is technical problems dealing with the high viscosity of the drug and the optical artifacts caused by the steep refractive gradient. The second challenge is the data analysis part, which involves hydrodynamic and thermodynamic non-ideality that need to be mathematically modeled.

There has been great progress in the last five to ten years on both the hardware and software [for AUC]. For example, 3D printed centerpieces now allow us to measure higher concentrations. Compared to other biophysical techniques, there aren't many alternatives available. Infrared spectroscopy can tell you about the folding but doesn't provide information about sizes. DLS (dynamic light scattering) only provides a weight-average size distribution and usually cannot separate monomers from dimers; you need eight times the mass of A to be separated from B.

So, AUC doesn't have many competitive technologies that can be used instead.

There has been some interest in finding new characterization methods for lipid nanoparticles (LNPs). In 2023, you published a paper on LNP characterization with the AUC. Can you elaborate on how AUC can be used for LNP characterization?

The idea, or let's say the application, was not invented by me. It was actually based on a publication by Amy Henrickson from Beckman Coulter Life Sciences. What we were interested in back then was whether we could analyze not only the size distribution and determine if there were empty particles left, but also if we could come up with an average number of mRNA copies per LNP. This largely determines the dose to be administered. Unlike siRNAs, which are very short and where you can only get an estimate in terms of 200-300 copies, with mRNA, due to its large size, you can get really precise single numbers. This was the main outcome of that investigation.

New Developments and Innovations:

Can you tell us about the new developments in the techniques you use for AUC? How do these improvements help in your research? What are the key considerations when optimizing AUC experiments for high-concentration formulations?

In my view, there have been two main areas of research and technical advancements in the field of AUC over the last 10 years. The first one is the introduction of multiwavelength capabilities with the new Optima AUC, which allows experiments to be conducted not only with two or three wavelengths, like with the ProteomeLab XLI plus interference optics, but also to obtain a third dimension of spectral information besides size and shape. This advancement was supported by software developments, especially in UltraScan and SEDANAL, for fitting these large data sets.

The second area is high-concentration AUC and the implementation of analysis tools for fitting for ks, kd, or second and third virial coefficients to describe self-association and non-ideality simultaneously. When optimizing high-concentration experiments, the main aspect you can optimize is the pathlength of the cell, which should be kept as short as possible to minimize optical artifacts. This is relatively simple and a matter of available hardware.

What's a bit trickier to balance is the rotor speed versus the duration of the experiment. If you spin too slowly, you get more diffusion and broader boundaries. On the other hand, if you centrifuge too quickly, you get very steep boundaries that cannot be captured by the interference camera. This balance needs to be determined empirically for each protein.

Future Directions and Impact:

What are the potential future uses of AUC in developing new biopharmaceuticals, especially those with high concentrations?

I would say the main area of improvement, or where AUC can really drive drug development, is in the formulation of high-concentration biopharmaceuticals. As mentioned before, viscosity is a huge problem. From an analytical perspective, this may be just annoying, but you need to remember that most of these solutions are IV preparations, which means they need to be injected into the patient. Higher viscosity prevents people from injecting it on their own, and if you inject a high-viscosity solution subcutaneously, it also creates a lot of pain. So, if you can reduce the viscosity by changing the formulation, it makes a huge difference for the patient.

Additionally, the kind of drugs and the concentration range that is accessible can be improved [for AUC]. Formulation development is conventionally done in these cases with DLS, but in my experiments, DLS is only useful up to a range of 30-50 mg/ml for antibodies. AUC allows scientists to analyze higher concentrations, you can easily screen dozens of buffers, unlike with chromatography. So, that's the area where I think AUC can really improve the development of high-concentration biopharmaceuticals.

How do you see the role of AUC changing in biopharmaceutical research over the next few years?

I see the biggest improvement for acceptance in the industry coming from a scientific perspective. Of course, I'm a little bit biased, but AUC is a great technology. What has prevented AUC from being widely adopted so far has been the compliance side, specifically GMP compliance. This has made a huge step forward with Lake Paul´s BASIS and specifically for the new Optima AUC, Borries Demeler's UltraScan GMP module. With this, you have AUC ready for release analytics and other QC routine testing. This indeed may help because it streamlines the analysis and requires less user interaction, which could spread the use of AUC in the industry.

Email: alexander.bepperling@sandoz.com

APPLICATION NOTE

Analytical Ultracentrifugation (AUC) for Characterization of Lipid Nanoparticles (LNPs): A Comprehensive Review

Amy Henrickson, Beckman Coulter

Lipid nanoparticles (LNPs) and liposomes (Figure 1) have revolutionized the medical field by serving as carriers for a wide range of therapeutic molecules, and have been used for cancer treatments, drug delivery, and vaccine development, including the recent COVID-19 mRNA vaccines by Moderna and Pfizer-BioNTech. mRNA cannot be injected directly into a patient due to its immunogenicity, toxicity, and susceptibility to RNase degradation and renal clearance[1]; however, by packaging the RNA into LNPs, these issues can be overcome. LNPs offer additional advantages, such as improved stability, targeted delivery, and adaptability to changing viral strains[2].

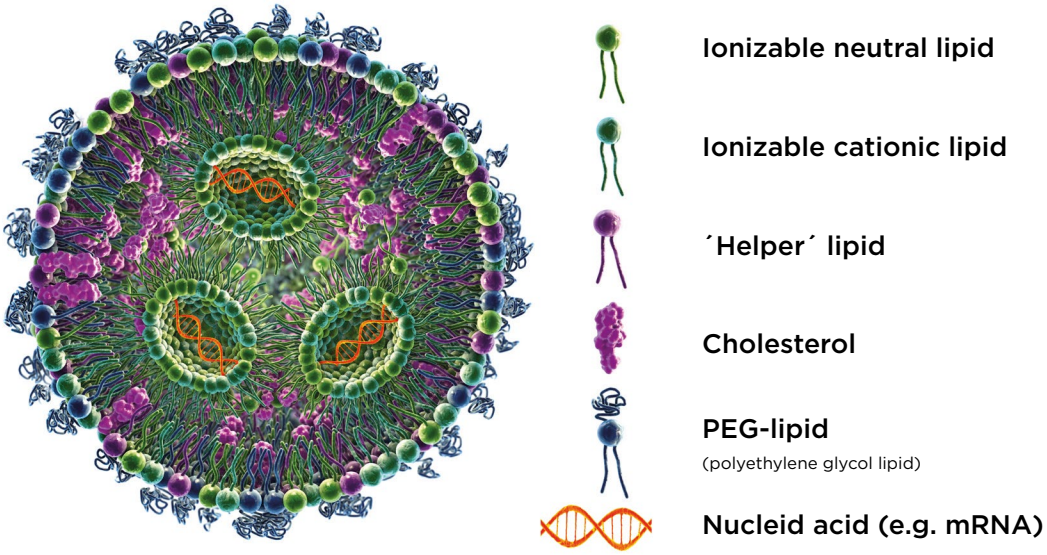

Figure 1: LNP´s
LNPs are small particles used in the pharmaceutical and biotechnology industries to help improve drug delivery. They are composed of a lipids which encapsulate the nucleic acid or other therapeutic agent, allowing for improved cell targeting and enhanced drug efficiency.

The biophysical characterization of LNPs is crucial for assessing their quality, efficacy, and safety. The accurate determination of size and homogeneity of LNP formulations is essential, as recent studies in model systems have demonstrated that they may influence the immunogenicity and potency of the treatment[3]; however, determining the accurate size distribution of an LNP formulation is difficult due to their inherent heterogeneity. Although dynamic light scattering (DLS) is commonly used for size determination, its measurements are based on Brownian motion, which limits the upper range of detection and, therefore may miss aggregates[4]. Additionally, DLS cannot differentiate between empty and loaded particles. To address these challenges, the FDA recommends employing orthogonal techniques for measurement[5]. Other important parameters to characterize include the free and bound/encapsulated cargo, the drug copy number distribution, the empty/full ratio of nanoparticles, and their stability.

Analytical ultracentrifugation (AUC) is a technology gaining traction for LNP characterization. When the samples are subjected to centrifugal forces, they are hydrodynamically separated based on their sedimentation coefficient (resulting from the analyte mass and density) and diffusion coefficient (resulting from particle shape). For LNPs, this can result in either sedimentation or flotation (Figure 2), depending on the lipid composition and cargo load. During centrifugation, an analyte's sedimentation/floatation and diffusion patterns are measured by tracking their absorption properties. From the measured sedimentation and diffusion parameters, size distributions, cargo loading, molar mass, and more can be determined for these challenging systems.

This review will examine how AUC has been used to characterize LNPs, and how it compares to other methodologies. Additionally, from these studies, it does not appear that the gravitational force generated during centrifugation affects the LNPs; if it did, this would be identifiable during analysis[6].

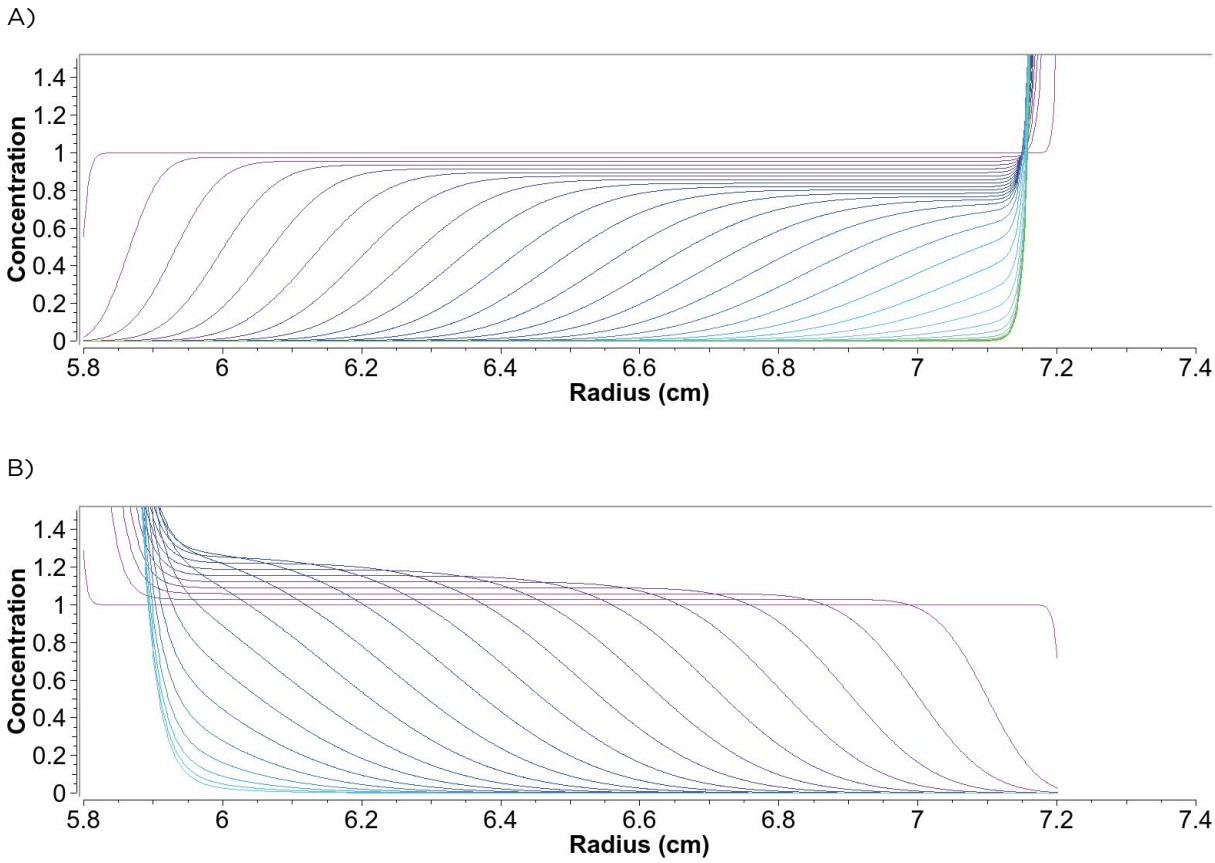

Figure 2: Examples of sedimenting and floating data collected on the AUC
Examples of the boundary shape of particles during centrifugation in the AUC. The earlier scans are depicted in purple and later scans in blue, then green. A) Depicts a sedimenting particle. B) Depicts a particle that floats during the centrifugation process.

Several studies have used AUC to determine size and size distribution of different LNP formulations, including siRNA, mRNA, and doxorubicin encapsulating systems[5–7]. These studies compared the average size and size distributions determined by AUC to techniques such as dynamic light scattering (DLS), nanoparticle tracking analysis (NTA), transmission electron microscopy (TEM), and asymmetrical-flow field-flow fractionation (AF4) in combination with multi-angle light scattering (MALS). The studies found that the average size determined by AUC corroborated well with all methods tested. Further, AUC could accurately determine the LNP size distributions for all formulations in agreement with AF4-MALS and Cryo-TEM. AF4-MALS and AUC provided high resolution when measuring and detecting samples with multiple polydisperse and high molecular weight species[5,8] (Figure 3). This is due to the ability of both methods to combine a separation technique and in-process detection. AUC also adds an additional dimension by separating the molecules based on size and density, resulting in accurate size distribution determinations for LNP samples.

Moreover, AUC has been used to study the free and bound cargo present in formulations[6,7], which is a critical parameter, as free cargo could result in toxicity and increased immune reactions[9]. The Optima AUC analytical ultracentrifuge contains a light source that can measure up to ~20 wavelengths between 190 – 800 nm in a single experiment. With this capability the adsorption of the cargo (e.g., 260 nm for nucleic acids and 490 nm for Doxil) can be measured through out the experiment. The LNP signal can also be detected, however, because lipids do not absorb light the signal measured is the scattered light from the LNPs. The scattering signal can typically be detected between 215-280 nm, depending on the size of the LNP. It should be noted that the scattering signal from the LNP will scale differently from the adsorption signal detected from the cargo[6]. By detecting the sample's sedimentation and diffusion patterns throughout the experiment, Mehn et al. calculated the amount of free drug present, and their results aligned well with HPLC and DLS measurements[7]. Henrickson et al. performed multiwavelength and fluorescence detection methods to show that their siRNA LNPs contained only encapsulated RNA[6].

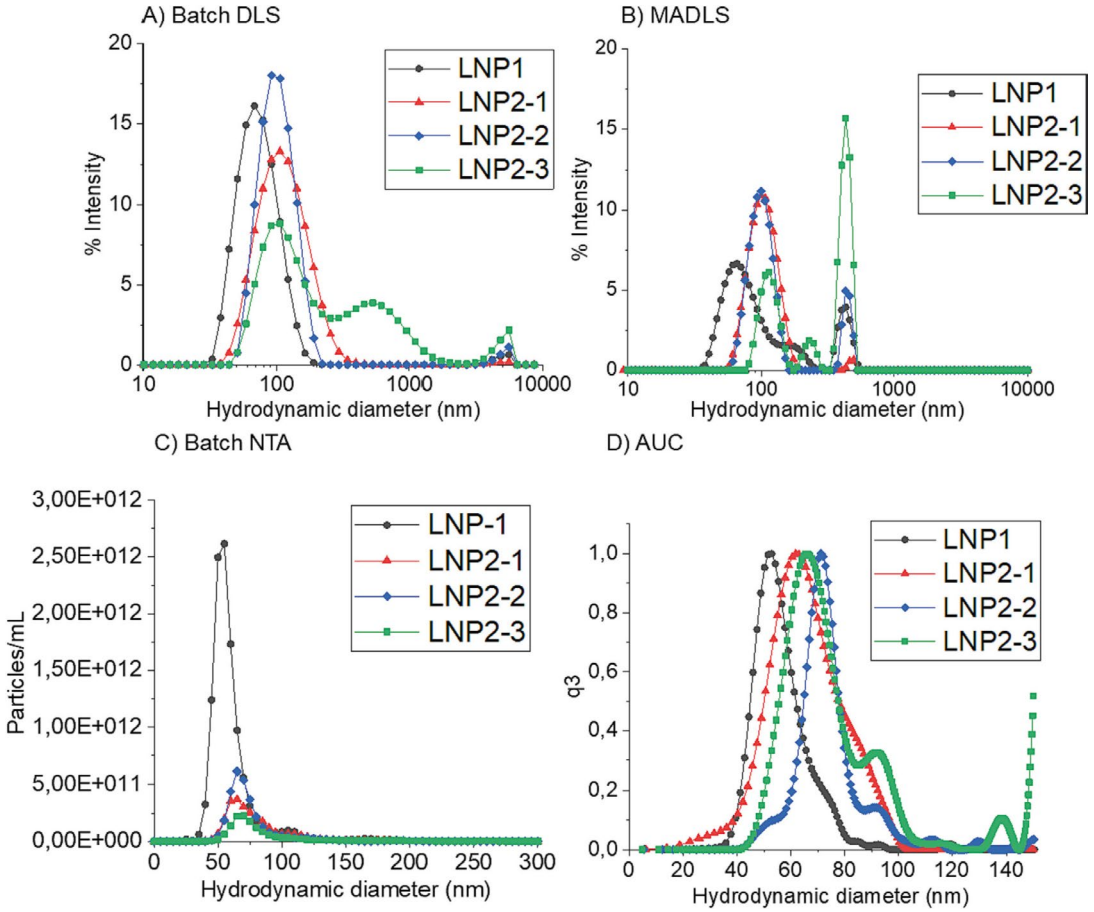

Figure 3: Hydrodynamic diameter of LNP formulations
Hydrodynamic diameter determination for four different LNP formulations measured by a) batch DLS, B) MADLS (multi-angle DLS), C) Batch NTA, and D) AUC. For more information and for an interpretation of the reference colors in the figure, see https://pubmed.ncbi.nlm.nih.gov/38253203/ Parot et al. DOI: 10.1016/j.jconrel.2024.01.037, Epub 2024, https://creativecommons.org/licenses/by/4.0/, image was not altered.

It is still unclear what role empty LNPs might play when or if they are administered during drug treatments; however, their characterization could help improve LNP production and ensure safe therapies. Using density matching AUC, where a sample is measured multiple times in buffers of different densities, it is possible to determine the density distribution of the entire sample[5–7]. Once the density distribution of the sample is known, it can be compared to an empty LNP sample. If an overlap in density is present, this could indicate that the sample contains a percentage of empty LNPs. Bepperling and Richter built on this method and used it to calculate the number of mRNA copies per capsid[10]. They found that their mRNA LNP formulation had a hydrodynamic radius distribution between 25 – 100 nm, and that it contained between 1 – 10 mRNA copy numbers per capsid. They determined that this single-digit value was plausible and in line with results from other studies of similarly sized LNPs[11–13]. These studies highlight the ability of AUC to characterize empty-full LNP distributions and mRNA payload capacity. Both are important parameters to consider, as they could impact cellular activities and mRNA expression kinetics,[12] and can help optimize LNP production and delivery of a wider range of therapeutics.

Finally, the stability of LNP formulations must be assessed at different time points while treating the samples according to conditions that will occur during real-life applications, such as freeze/thaws and manipulation at room temperature[9]. Thaller et al. compared AUC and DLS to characterize LNP polydispersity and stability under different stress conditions[8]. DLS could qualitatively determine the hydrodynamic radius and identify changes in the formulations when exposed to freeze/thaw and mechanical stress, but not heat stress, at 50°C. They determined that AUC was a quantitative characterization method for LNPs that could provide more precise particle size distributions, identify changes in all tested stress conditions, and observe changes in particle density, which DLS cannot detect.

These studies highlight the versatility and utility of AUC for the characterization of LNP formulations. AUC can precisely determine the size distribution of LNP formulations in agreement with AF4-MALS and TEM. In addition, it can identify and quantify the presence of free cargo and empty LNPs in solution and can be used to determine the number of mRNA copies per LNP. Overall, AUC is a quantitative, first-principle method that is non-destructive, provides a comprehensive and reliable approach to the characterization of LNPs, and has become an indispensable tool in LNP research.

Citations:

1. Yin H, Kanasty RL, Eltoukhy AA, Vegas AJ, Dorkin JR, Anderson DG. Non-viral vectors for gene-based therapy. Nat Rev Genet. 2014 Aug;15(8):541–55.
2. Corbett KS, Edwards DK, Leist SR, Abiona OM, Boyoglu-Barnum S, Gillespie RA, et al. SARS-CoV-2 mRNA vaccine design enabled by prototype pathogen preparedness. Nature. 2020 Oct;586(7830):567–71.
3. Chen L, Ge B, Casale FP, Vasquez L, Kwan T, Garrido-Martín D, et al. Genetic drivers of epigenetic and transcriptional variation in human immune cells. Cell. 2016 Nov 17;167(5):1398-1414.e24.
4. Caputo F, Vogel R, Savage J, Vella G, Law A, Della Camera G, et al. Measuring particle size distribution and mass concentration of nanoplastics and microplastics: addressing some analytical challenges in the sub-micron size range. J Colloid Interface Sci. 2021 Apr 15;588:401–17.
5. Parot J, Mehn D, Jankevics H, Markova N, Carboni M, Olaisen C, et al. Quality assessment of LNP-RNA therapeutics with orthogonal analytical techniques. J Control Release. 2024 Mar;367:385–401.
6. Henrickson A, Kulkarni JA, Zaifman J, Gorbet GE, Cullis PR, Demeler B. Density Matching Multi-wavelength Analytical Ultracentrifugation to Measure Drug Loading of Lipid Nanoparticle Formulations. ACS Nano. 2021 Mar 23;15(3):5068–76.
7. Mehn D, Iavicoli P, Cabaleiro N, Borgos SE, Caputo F, Geiss O, et al. Analytical ultracentrifugation for analysis of doxorubicin loaded liposomes. Int J Pharm. 2017 May 15;523(1):320–6.
8. Thaller A, Schmauder L, Frieß W, Winter G, Menzen T, Hawe A, et al. SV-AUC as a stability-indicating method for the characterization of mRNA-LNPs. Eur J Pharm Biopharm. 2023 Jan;182:152–6.
9. Guerrini G, Magrì D, Gioria S, Medaglini D, Calzolai L. Characterization of nanoparticles-based vaccines for COVID-19. Nat Nanotechnol. 2022 Jun 16;17(6):570–6.
10. Bepperling A, Richter G. Determination of mRNA copy number in degradable lipid nanoparticles via density contrast analytical ultracentrifugation. Eur Biophys J. 2023 Jul;52(4–5):393–400.
11. Sabnis S, Kumarasinghe ES, Salerno T, Mihai C, Ketova T, Senn JJ, et al. A Novel Amino Lipid Series for mRNA Delivery: Improved Endosomal Escape and Sustained Pharmacology and Safety in Non-human Primates. Mol Ther. 2018 Jun 6;26(6):1509–19.
12. Li S, Hu Y, Li A, Lin J, Hsieh K, Schneiderman Z, et al. Payload distribution and capacity of mRNA lipid nanoparticles. Nat Commun. 2022 Sep 23;13(1):5561.
13. Carrasco MJ, Alishetty S, Alameh M-G, Said H, Wright L, Paige M, et al. Ionization and structural properties of mRNA lipid nanoparticles influence expression in intramuscular and intravascular administration. Commun Biol. 2021 Aug 11;4(1):956.

WHITEPAPER

Enhancing Molecular Studies with Multiwavelength Analytical Ultracentrifugation

Amy Henrickson, Beckman Coulter Life Sciences
Sameera Qureshi, Beckman Coulter Life Sciences

Introduction

In the realm of analytical ultracentrifugation (AUC) instruments, the integration of multiwavelength (MW) analysis has emerged as a groundbreaking approach for elucidating the interactions between multiple molecules with distinct absorbance profiles.[7] The Optima AUC Analytical Ultracentrifuge from Beckman Coulter Life Sciences, equipped with Rayleigh interference optics and multiwavelength-capable UV/visible absorption optics (collectively known as "Beckman optics"), epitomizes this technological advancement.[6]

This white paper delves into the principles and applications of multiwavelength analytical ultracentrifugation (MW-AUC) as an advanced method for studying biopolymer interactions under physiological conditions. Through a series of research experiments, we illustrate the efficacy of the Optima AUC in characterizing molecular interactions across various biological systems, including enzyme activity, viral vectors, protein-DNA interactions, biopolymer mixtures and lipid nanoparticles.

MW-AUC enables the study of biopolymer interactions in a physiological environment, where factors such as ionic strength, pH and redox potential can be precisely controlled.[6] This technique measures samples while separating them using centrifugal force, allowing for high-resolution characterization of the different analytes in the solution. MW-AUC is particularly beneficial when the solution contains analytes with distinct absorbance spectra. By collecting data at multiple wavelengths, analytes can be differentiated based on variations in their hydrodynamic properties and absorbance characteristics. If the pure spectra of the individual analytes are known, the MW-AUC data can be decomposed into the pure spectra. This allows for the determination of stoichiometry and molar ratio for each analyte in solution.[6]

MW-AUC has advanced the analysis of various interacting systems, including protein-DNA,[2,3] protein-RNA,[4] biopolymers,[5] heme proteins and amyloid-ß peptide interactions,[6] as well as the characterization of AAVs,[1,7,8,9] Its capability to determine DNA insert length and wavelength-specific correction factors for different insert sizes has been demonstrated.[8] Below, we present a few research experiments that were carried out using the Optima AUC and discuss how multiwavelength experiments helped scientists to further their research.

I. Biopolymer mixtures and interactions

To highlight the overall utility of MW-AUC, Henrickson et al.[14] highlights two different examples. In the first, they look at an oilseed protein extract where the spectral properties of each analyte in solution are unknown, and in the second case, they look at a mixture of three proteins, where the pure spectral signature of each protein is known. In the oilseed protein extract, they employed MW-AUC to study and identify the components of the extract. The extract contained water-soluble polyphenols (315 nm absorbance peak) and proteins of unknown size. They wanted to determine if the polyphenols were bound to the proteins in the solution or remained free in the solution. MW-AUC revealed that most polyphenols sedimented at ~0.5–1.0 S, while the primary protein (12.5 S) remained intact with no polyphenol interaction, whereas a smaller protein fraction (<2S) suggested degradation with possible polyphenol binding. This study highlights that even if an optical deconvolution cannot be performed because the pure basis spectra are unknown, MW-AUC can still help to elucidate the answer by highlighting the spectral difference at each sedimentation coefficient.

II. Protein-DNA interactions

Ahmed et al.[13] used AUC to investigate the interaction between DNA and ComEA, a critical protein in bacterial transformation. During transformation, DNA uptake into the periplasm is facilitated by type IV pili, which bind and retract DNA, while ComEA, a highly conserved DNA-binding protein, functions as a Brownian ratchet, driving the translocation of transforming DNA into the periplasm. They used AUC and X-ray crystallography to help elucidate the function of one domain on ComEA and used MW-AUC to investigate the interaction between DNA and the ComEA DNA-binding domain.

X-ray crystallography found that the unknown domain on ComeEA appeared to be involved in the oligomerization formation of the proteins. AUC was used to confirm that this oligomerization occurred in solution and determine if it was reversible, and the results confirmed a monomer-dimer equilibrium with a K_D of 33.8 μM. Thus, the domain was called the oligomerization domain (OD). It was speculated that this OD also played an important role in ComEA binding to DNA. To test this, a mutant, ComEA-A108Y, was created, which prevents the oligomerization. Using MW-AUC, the researchers could confirm the total number of ComEA proteins binding to the DNA and identified that almost twice as many ComEA wild-type proteins could bind the DNA compared to ComEA-A108Y. The utility of the ComEA oligomerization process appears to facilitate the efficient and cooperative packing of ComEA on DNA, which is crucial for its function in bacterial transformation.

Horne et al.[15] investigated the interactions between NanR dimers and between NanR and DNA. NanR, a transcription repressor, regulates sialic acid metabolism in *Escherichia coli*. Sialic acid coats human cell surfaces and serves as a nutrient source for both pathogenic and commensal bacteria. Their study demonstrated, using cryo-electron microscopy and MW-AUC, that three NanR dimers cooperatively and with high affinity bind to a $(GGTATA)_3$ repeat operator, providing a molecular basis for the regulation of bacterial sialic acid metabolism.

The researchers titrated NanR against the DNA repeat operator and measured the different titrations using MW-AUC recording scans within the 220-300 nm range at 2 nm increments. They then deconvoluted the sedimentation signal into the individual protein and DNA spectral signals, and could identify the NanR and DNA peaks co-migrating, indicating an interaction. At low NanR concentrations, a free DNA peak is also present (Fig. 1b), and as the NanR concentration was increased, the free DNA decreased. At the highest concentration, a free NanR peak appears, indicating saturation of the DNA (Fig. 1e). Due to the optical deconvolution, the researchers could also determine the number of NanR binding to the DNA at each titration, with a final molar ratio of NanR to DNA of 6.44:1, consistent with three NanR-dimer binding to the DNA. This study provided molecular insights into the regulatory mechanism governing bacterial sialic acid metabolism.

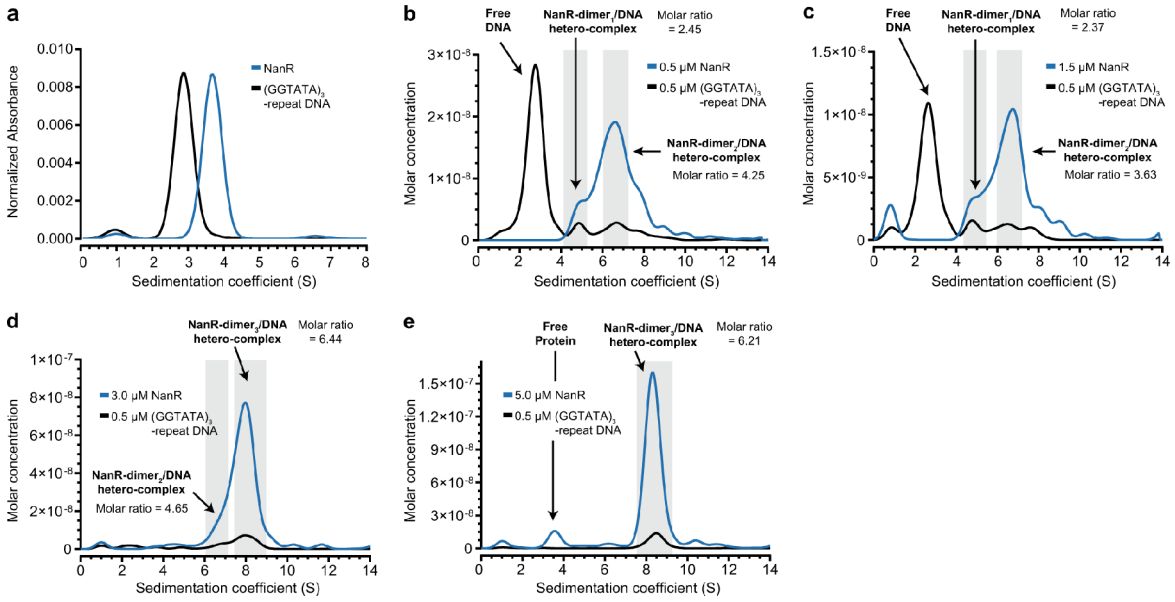

Figure 1. a: *Sedimentation coefficient distributions of the NanR (blue) and the (GGTATA)3-repeat DNA operator (black) controls, measured individually at 280 and 260 nm, respectively. b–e: Deconvoluted sedimentation coefficient distributions resulting from the titration of NanR into (GGTATA)3-repeat DNA (0.5 μM): 0.5 μM NanR (b), 1.5 μM NanR (c), 3.0 μM NanR (d), and 5.0 μM NanR (e). A shift in the sedimentation coefficient is observed with increasing NanR concentration, consistent with hetero-complex formation. The molar ratio of the integrated peaks (shaded in gray) and the oligomeric state of each hetero-complex is shown. The presence of excess protein free of any co-migrating DNA in e indicates that hetero-complex formation has reached saturation. All plots are presented as g(s) distributions with the molar concentration for each interacting partner (protein and DNA) plotted on the y-axis.*

III. Viral vectors and MW-AUC

AUC has established itself as the gold standard method for adeno-associated virus (AAV) characterization, as it can characterize and quantify the different loading states of the viral particles as well as contaminants, including overfilled particles, aggregates and degradants. **Maruno et al.**[12] present an effective methodology for size distribution analysis and AAV vector loading states. This precise assessment is essential, as product-related impurities —including empty particles (EPs), intermediate particles (IPs) and aggregates—may reduce therapeutic efficacy and exacerbate undesirable immune responses. Using band sedimentation analytical ultracentrifugation (BS-AUC) with multiwavelength detection on the Optima AUC (Beckman Coulter Life Sciences), this approach enables precise separation of full particles (FPs), EPs, and IPs using a small amount of samples. The total peak area of the sedimentation coefficient distribution obtained from BS-AUC analysis corresponded with absorbance measurements determined via ultraviolet-visible (UV-Vis) absorption spectroscopy.

AAV loading state identification was achieved in MW-BS-AUC by analyzing the wavelength dependence of the c(s) peak area, which corresponded to the spectral profile of each component. Additionally, minor peak identification was performed with greater precision and reliability using multiwavelength sedimentation velocity analytical ultracentrifugation (MW-SV-AUC). These approaches serve as a powerful analytical tool for AAV vector production process development, as well as for batch-to-batch and lot-to-lot quality assessments of AAV drug substances.

Henrickson et al.[7] present MW-AUC as a highly accurate method for the characterization and quantification of AAV samples. The results were compared with dual-wavelength AUC, transmission electron microscopy, and mass photometry. Unlike dual-wavelength AUC, MW-AUC provides precise quantification of AAV capsid ratios and enables the identification of contaminants. In contrast to transmission electron microscopy, MW-AUC also detects and quantifies partially filled capsids. Furthermore, unlike mass photometry, MW-AUC yields first-principle results. This study highlights the enhanced analytical capabilities of MW-AUC, emphasizing the utility of recently integrated UltraScan programs and reaffirming AUC as the gold standard for viral vector analysis.

Richter et al.[8] demonstrated the capability of MW-AUC to determine DNA insert length and derive wavelength-specific correction factors for varying insert sizes. The study compared biophysical methods for assessing the purity and DNA content of viral capsids across five AAV serotypes using multiwavelength detection at 230 nm, 260 nm and 280 nm. MW-AUC was employed to quantify species content and derive wavelength-specific correction factors for respective insert sizes.

At each detection wavelength—230 nm, 260 nm, 280 nm, and Rayleigh interference—empty, filled, and partially filled capsids were identified. In mixed populations analyzed using multiwavelength approaches, the measured contents varied by wavelength due to differences in extinction coefficients between empty and filled capsids. The results were further validated through comparisons with multiple orthogonal characterization methods, which produced consistent findings on empty and filled capsid content. While anion-exchange chromatography (AEX) and UV spectroscopy can quantify empty and filled AAVs, only SV-AUC successfully detected low levels of partially filled capsids.

The study demonstrated that modeling and confirming response factors for native AAVs with differently sized DNA constructs is now feasible due to the high resolution of SV-AUC. Additionally, SV-AUC enables precise determination of specific absorbance ratios, response factors and extinction coefficients for each capsid type, establishing it as the highest-resolution technique among those evaluated.

Conclusion

The application of MW-AUC using the Optima AUC from Beckman Coulter Life Sciences has significantly advanced our understanding of complex molecular interactions. The research examples presented herein underscore the versatility and precision of MW-AUC in various scientific inquiries, from enzyme regulation and viral vector characterization to protein-DNA binding dynamics and the analysis of biopolymer mixtures. The integration of MW-AUC into analytical workflows not only enhances the accuracy of molecular studies but also reaffirms its status as an indispensable tool in the field of life sciences, offering unparalleled analytical capabilities and contributing to the progression of molecular biology, virology and biochemistry.

References

1. Maruno T, Usami K, Ishii K, Torisu T, Uchiyama S. Comprehensive Size Distribution and Composition Analysis of Adeno-Associated Virus Vector by Multiwavelength Sedimentation Velocity Analytical Ultracentrifugation. J Pharm Sci. 2021 Oct;110(10):3375–3384. PMID: 34186069
2. Ahmed I, Hahn J, Henrickson A, Khaja FT, Demeler B, Dubnau D, Neiditch MB. Structure-function studies reveal ComEA contains an oligomerization domain essential for transformation in gram-positive bacteria. Nat Commun. 2022 Dec 13;13(1):7724. PMCID: PMC9747964
3. Horne CR, Venugopal H, Panjikar S, Wood DM, Henrickson A, Brookes E, North RA, Murphy JM, Friemann R, Griffin MDW, Ramm G, Demeler B, Dobson RCJ. Mechanism of NanR gene repression and allosteric induction of bacterial sialic acid metabolism. Nat Commun. 2021 Mar 31;12(1):1988.
4. Zhang J, Pearson JZ, Gorbet GE, Cölfen H, Germann MW, Brinton MA, Demeler B. Spectral and Hydrodynamic Analysis of West Nile Virus RNA-Protein Interactions by Multiwavelength Sedimentation Velocity in the Analytical Ultracentrifuge. Anal Chem. 2017 Jan 3;89(1):862–870. PMCID: PMC5505516
5. Johnson CN, Gorbet GE, Ramsower H, Urquidi J, Brancaleon L, Demeler B. Multi-wavelength analytical ultracentrifugation of human serum albumin complexed with porphyrin. Eur Biophys J. 2018 Oct;47(7):789–797. PMCID: PMC6158097
6. Henrickson A, Gorbet GE, Savelyev A, Kim M, Hargreaves J, Schultz SK, Kothe U, Demeler B. Multi-wavelength analytical ultracentrifugation of biopolymer mixtures and interactions. Anal Biochem. 2022 Sep 1;652:114728. PMCID: PMC10276540.
7. Henrickson A, Ding X, Seal AG, Qu Z, Tomlinson L, Forsey J, Gradinaru V, Oka K and Demeler B. Characterization and quantification of adeno-associated virus capsid-loading states by multi-wavelength analytical ultracentrifugation with UltraScan. Nanomedicine (Lond). 2023;18(22):1519-1534. doi: 10.2217/nnm-2023-0156. Epub 2023 Oct 25.
8. Richter K, Wurm C, Strasser K, Bauer J, Bakou M, VerHeul R, Sternisha S, Hawe A, Salomon M, Menzen T, Bhattacharya A. Purity and DNA content of AAV capsids assessed by analytical ultracentrifugation and orthogonal biophysical techniques. Eur J Pharm Biopharm. 2023:189:68-83. doi:10.1016/j.ejpb.2023.05.011.
9. Bepperling A, Best J. Comparison of three AUC techniques for the determination of the loading status and capsid titer of AAVs. Eur Biophys J. 2023 Jul;52(4-5):401-413. doi: 10.1007/s00249-023-01661-0. Epub 2023 May 28. PMID: 37245172. doi: 10.1007/s00249-023-01661-0.
10. Henrickson A, Kulkarni JA, Zaifman J, Gorbet GE, Cullis PR, Demeler B. Density Matching Multi-wavelength Analytical Ultracentrifugation to Measure Drug Loading of Lipid Nanoparticle Formulations. ACS Nano. 2021 Mar 23;15(3):5068–76.
11. Potter JR, Rivera S, Young PG, Patterson DC, Namitz KE, Yennawar N, Kincaid JR, Liu Y, Weinert EE. Heme pocket modulates protein conformation and diguanylate cyclase activity of a tetrameric globin coupled sensor. Journal of Inorganic Biochemistry, 258, 2024, 112638, ISSN 0162-0134, https://doi.org/10.1016/j.jinorgbio.2024.112638.
12. Maruno T, Ishii K, Torisu T, Uchiyama S. Size Distribution Analysis of the Adeno-Associated Virus Vector by the c(s) Analysis of Band Sedimentation Analytical Ultracentrifugation with Multiwavelength Detection. Journal of Pharmaceutical Sciences, 112(4), 2023, 937-946. https://doi.org/10.1016/j.xphs.2022.10.023.
13. Ahmed I, Hahn J, Henrickson A. et al. Structure-function studies reveal ComEA contains an oligomerization domain essential for transformation in gram-positive bacteria. Nat Commun 13, 7724 (2022). https://doi.org/10.1038/s41467-022-35129-0.
14. Henrickson A, Gorbet GE, Savelyev A, Kim M, Hargreaves J, Schultz SK, Kothe U, Demeler B. Multi-wavelength analytical ultracentrifugation of biopolymer mixtures and interactions. Analytical Biochemistry, 652, 2022. https://doi.org/10.1016/j.ab.2022.114728.
15. Horne CR, Venugopal H, Panjikar S. et al. Mechanism of NanR gene repression and allosteric induction of bacterial sialic acid metabolism. Nat Commun 12, 1988 (2021). https://doi.org/10.1038/s41467-021-22253-6.
16. Henrickson A, Kulkarni JA, Zaifman J, Gorbet GE, Cullis PR, Demeler B. Density Matching Multi-wavelength Analytical Ultracentrifugation to Measure Drug Loading of Lipid Nanoparticle Formulations. ACS Nano. 2021 Mar 23;15(3):5068–76.
17. Mehn D, Iavicoli P, Cabaleiro N, Borgos SE, Caputo F, Geiss O, et al. Analytical ultracentrifugation for analysis of doxorubicin loaded liposomes. Int J Pharm. 2017 May 15;523(1):320–6.

For Beckman Coulter's worldwide office locations and phone numbers, please visit Contact Us at beckman.com
2025-GBL-EN-107480-v1

Further reading and resources

Learn more about AUC:
Analytical Ultracentrifugation (AUC)

Whitepaper:
Analytical Ultracentrifugation: A Versatile and Valuable Technique for Macromolecular Characterization

AUC Experimental Types:
https://www.beckman.com/resources/technologies/analytical-ultracentrifugation/experiments

WILEY

Imprint

Senior Account Manager: Joseph Tomaszewski

Editor: Dr. Christene A. Smith

2025-GBL-EN-107589-v1